$(e,2e)$ study of cadmium ionization in the $4d^9 5s^2 5p$ autoionizing region

N. L. S. Martin,[1] R. P. Bauman,[1] and M. Wilson[2]
[1]*Department of Physics and Astronomy, University of Kentucky, Lexington, Kentucky 40506-0055*
[2]*Physics Department, Royal Holloway, University of London, Egham, Surrey TW20 0EX, United Kingdom*
(Received 4 February 1998; revised manuscript received 9 November 1998)

Cadmium $(e,2e)$ energy spectra have been measured for incident electron energy 150 eV and scattering angles 2°–18°, corresponding to momentum transfer 0.2–1 a.u. This choice of kinematics covers the transition from the dipole limit at 0.2 a.u. to the binary collisions regime at 1 a.u. The data are presented as the sum and difference of pairs of $(e,2e)$ spectra with ejected-electron directions 180° apart. This analysis reveals trends in the data and also provides a sensitive test of theory. Data sets for three special ejected-electron directions are compared with plane-wave Born approximation calculations. The calculated spectral shapes are in good agreement with all experiments when a simple phase correction is incorporated. The calculated difference/sum relative intensities are in good agreement with one data set but are in very poor agreement with the other two. [S1050-2947(99)02804-8]

PACS number(s): 34.80.Dp, 32.80.Dz

I. INTRODUCTION

In this paper we present a comprehensive set of experiments on electron-impact ionization of a system where both nonresonant and resonant processes are important. Here, the former process corresponds to the direct ejection of an electron, whereas the latter involves intermediate autoionizing states. Photoionization involving autoionization is well known and understood: energy eigenstates are admixtures of discrete and continuum configurations, and interferences between direct and indirect processes result in asymmetric Fano line shapes [1]. Less well understood are the interferences between orthogonal resonant and nonresonant channels that are coherently populated as a result of charged particle-impact ionization.

Detailed information about such processes can be obtained by the electron-electron coincidence, or $(e,2e)$, technique in which an atomic beam is crossed with an electron beam. Following ionization, the two outgoing electrons (1 and 2) are detected in (delayed) coincidence at predetermined angles and energies, subject to the energy balance $E_0 = E_1 + E_2 + IP$, where IP is the threshold energy of the chosen final ion state. Several groups have carried out $(e,2e)$ experiments on helium in the $2l2l'$ autoionizing region [2,3]. The experiments are difficult because of the small ionization cross sections; theoretical interpretations are difficult because helium is an extremely correlated system, which affects, for example, the excitation mechanism for $1s^2 \rightarrow 2l2l'$.

Paradoxically, cadmium, with 48 electrons and ground state $4d^{10}5s^{2\,1}S_0$, is a ''simpler'' system. The low-energy ejected-electron spectrum is dominated by the $4d^9 5s^2 5p$ autoionizing levels, the gross features of which are well described in the single configuration independent-particle approximation [4,5]. Excitation occurs via the optically allowed single-particle transition $4d \rightarrow 5p$ with a cross section two orders of magnitude larger than those of the helium autoionizing levels [6]. Thus under similar experimental conditions, data with statistics ten times better than those of helium $(e,2e)$ experiments can be obtained with the same run times.

In previous work in cadmium we determined relative magnitudes and phases of monopole, resonant dipole, and quadrupole ionization amplitudes (i.e., $J = 0,1,2$ partial wave amplitudes), from $(e,2e)$ experiments carried out with kinematic conditions corresponding to small momentum transfer $K \sim 0.2$ a.u. [7,8]. The experiments measured $(e,2e)$ energy spectra at carefully chosen pairs of ejected-electron directions 180° apart; the experimental data were presented as the sum and difference of each spectral pair. The difference spectrum isolated the interference cross terms, which are implicit functions of complex ionization amplitudes. Magnitudes *and* phases may be obtained from such interference spectra because the energy-dependent ejected-electron phase increases by π across an autoionizing resonance in a well-defined manner. The extra (approximately energy independent) phase due to scattering may then be extracted from the shape of the observed interference spectrum, and the size of the interference spectrum yields the magnitude of the ionization amplitude. Details of this technique are given in Refs. [7] and [8]. It was found that for $J = 0,1,2$ ionization amplitudes, the relative magnitudes differ by about a factor of 2, and that relative phases differ by about $\pi/4$, from a plane-wave Born approximation (PWBA) calculation. A recent distorted wave Born approximation (DWBA) calculation is not in any better agreement with the experimental data [9].

The interference effects at small momentum transfer represent small deviations from the dipole approximation; i.e., the experiments were carried out close to the dipole limit. [In fact, even in true Cd photoionization experiments, dipole-quadrupole interference effects can be detected, albeit two orders of magnitude smaller in size than in the $(e,2e)$ experiments [10].] We have now extended our $(e,2e)$ measurements to cover a momentum transfer range up to 1 a.u., where this is no longer the case. The experiments are of interest because the range $K = 0.2 \rightarrow 1$ a.u. covers the transition from the dipole to the binary collision region. Thus our experiments show the transition from the photoionization limit of $(e,2e)$ to the limit where the collision process must

TABLE I. Cadmium autoionizing levels (above the 8.99-eV ionization potential) labeled by their largest *LS* component. Most of the $J=1$ level energies are known experimentally. All other levels are *ab initio* calculated values, adjusted to give a tolerable fit to our data. The $J=3$ data are from Ref. [18]; *LS* coupling is inappropriate for these levels. The $5p^2$ widths are from matrix elements calculated at the $5p6p$ configuration average energy; these differ somewhat from the local values.

			Energy (eV)	Width (eV)
$J=0$	$5p^2$	^3P	0.18	0.0007
		^1S	1.94	0.058
	$5p6p$	^3P	3.69	0.0001
		^1S	4.12	0.0014
	$5p7p$	^3P	4.49	0.0001
		^1S	4.77	0.0005
$J=1$	$4d^9 5s^2 5p$	^3P	3.07	0.041
		^1P	3.81	0.140
		^3D	3.94	0.003
	$5p6s$	^3P	2.87	0.054
		^1P	3.19	0.273
	$5p5d$	^3D	3.86	0.003
		^3P	4.03	0.008
		^1P	4.22	0.015
	$5p7s$	^3P	4.34	0.015
		^1P	4.53	0.088
	$5p8s$	^3P	4.82	0.021
		^1P	5.07	0.042
$J=2$	$5p^2$	^3P	0.37	0.019
		^1D	0.88	0.767
	$5p6p$	^3D	3.70	0.009
		^3P	3.98	0.023
		^1D	4.09	0.130
	$5p7p$	^3D	4.54	0.025
		^3P	4.79	0.012
		^1D	4.86	0.098
$J=3$	$4d^9 5s^2 5p$	-	2.80	0.006
		-	3.33	0.0002
		-	3.77	0.004

be analyzed in terms of charged-particle scattering. For these kinematics a partial wave analysis of the ejected electron cannot be terminated at $J=2$ and therefore it is not possible to extract individual multipole amplitudes. However, for reasons given below, we will still present the data as the sum and difference of (*e*,2*e*) energy spectra, as in the previous work. In the absence of any more sophisticated theory, we compare our experimental results with PWBA calculations.

The calculations are discussed in Sec. II. Section III gives experimental details, and Secs. IV and V give the experimental results and the conclusions.

II. THEORY

One approach to the analysis of (*e*,2*e*) energy spectra is to fit a generalized line profile [11,12] to individual spectra and compare the fit parameters with calculated values. This method only applies to the case of noninterfering overlapping resonances, and is therefore not suitable for an analysis of our cadmium data where there is very strong interaction among the overlapping $J=1$ resonances [5].

The analysis of our earlier small momentum transfer data was based on a model constructed using the PWBA. Although a quantitative comparison of experimental and PWBA ionization amplitudes showed disagreement, one of the cornerstones of the theory, the special role of the momentum transfer axis, appeared to be validated by observations made at special ejected-electron directions with respect to this axis. In the present experiments at larger momentum transfer this axis is expected to have less significance. Nevertheless, our discussion of the analysis and presentation of the new data will be framed in the context of the PWBA since this illustrates the salient points. What follows is based on the theory given in Ref. [8] but without the restriction of small momentum transfer.

We wish to describe, with a PWBA model, the overall electron-impact ionization process

$$\mathrm{Cd}(5s^2\,{}^1S_0)+e_0\rightarrow \mathrm{Cd}^+(5s\,{}^2S_{1/2})+e_{\mathrm{ej}}+e_{\mathrm{sc}}, \qquad (1)$$

in the region dominated by the $4d^9 5s^2 5p$ autoionizing resonances [6].

We shall ignore electron exchange scattering, in which case the (slow) ejected electron and the (fast) scattered electron are distinguishable (exchange is discussed elsewhere [13]). Thus an electron of incident momentum $\vec{k}$ is scattered through an angle θ_{sc} with final momentum $\vec{k}'$ and momentum transfer $\vec{K}=\vec{k}-\vec{k}'$. The ionized electron is ejected with energy E and momentum $\vec{k}_{\mathrm{ej}}$. The final asymptotic ion plus ejected-electron state $|f\rangle$, corresponding to an ejected electron of energy E at the detector (i.e., $r\rightarrow\infty$), is represented as a coherent superposition of continua which are total angular momentum and energy eigenstates

$$|f\rangle=\sum_{LSJM} c_{LSJM}|5sElLSJM\rangle, \qquad (2)$$

where the c_{LSJM} are complex coefficients that contain the Jth multipole amplitude from the $^1S_0$ ground-state neutral. The exclusion of basis states with energies $\neq E$ is equivalent to neglecting any effects due to post-collision interaction (PCI), a semiclassical description in which the scattered electron interacts with the ejected electron after the ''quantum-mechanical'' collision leading to a ''classical'' exchange of energy [14].

In the PWBA the summation can be reduced by choosing the quantization axis along the direction of momentum transfer $\hat{K}$, in which case $M=0$ only [15]. Parity unfavored processes [16], due to the presence of intermediate-coupled Cd autoionizing states [4], may result in the population of triplet continua in addition to the singlet continua allowed by PWBA direct ionization. In terms of *LS*-coupled continua, the allowed final states are $5sEl\,{}^{2S+1}L_J$, where $l=L=J$ and $S=0$ or 1; from Eq. (2) it can be seen that there is thus a direct correspondence between a multipole expansion of the

TABLE II. Parameters of the coplanar $(e,2e)$ experiments carried out with 150-eV incident electron energy. The first three columns give the general kinematics; the last three columns list the actual angles for each experiment: momentum transfer (MT), P_2 magic angle, and P_3 magic angle. Scattering angles are positive (negative) for angles measured in a clockwise (counterclockwise) direction from the incident beam direction. Ejected electron angles (both on the binary and recoil sides) are all given as positive and are measured in a counterclockwise direction from the incident beam. All kinematics are evaluated for the $4d^9 5s^2 5p\,^1P_1$ energy level. The scattered and ejected electron detectors would overlap for a P_2 experiment at $\theta_{sc}=18°$.

			$\theta_{sc}/\theta_{ej}^{bin}/\theta_{ej}^{rec}$		
θ_{sc}	K	θ_K	MT	P_2	P_3
2	0.18	36		+2/90/270	
3	0.22	47	+3/50/230		+3/90/270
4.5	0.29	58	+4.5/58/238	−4.5/248/68	−4.5/264/84
6	0.37	64	+6/64/244	−6/242/62	−6/257/77
7.5	0.44	67	+7.5/67/247	−7.5/238/58	−7.5/254/74
9	0.53	69	+9/69/249	−9/236/56	−9/251/71
12	0.69	72	+12/72/252	−12/233/53	−12/249/69
15	0.86	73	+15/73/253	−15/233/53	−15/248/68
18	1.02	73	+18/73/253		−18/247/67

scattering amplitude and a partial wave expansion of the ejected-electron wave function.

The angular distribution of electrons ejected with energy E, measured in coincidence with electrons scattered through an angle θ_{sc}, is given by a coherent sum over J but an incoherent sum over S [8]:

$$I(\theta_{sc};E,\hat{k}_{ej}) \sim \sum_{S=0}^{1} \left| \sum_{J} b_{JS}(\theta_{sc},E) Y_{JS}(\hat{k}_{ej}) \right|^2, \qquad (3)$$

where $Y_{JS}(\hat{k}_{ej})$ is a spherical harmonic whose argument is evaluated with respect to the momentum transfer direction. The complex coefficients describe the ionization process and incorporate the total phase as described below.

$(e,2e)$ spectra taken for opposite ejected-electron directions (along $+\vec{k}_{ej}$ and $-\vec{k}_{ej}$) differ because the parity of the cross terms $Y_{JS}Y^*_{J'S}$ is given by $(-1)^{(J+J')}$. We shall denote such pairs of spectra I^+ and I^-, where the positive (negative) sign refers to the binary (recoil) side of the electron beam axis.

The *sum* and *difference* spectra are then

$$(I^+ + I^-) \sim \sum_{S=0}^{1} \sum_{J} |b_{JS} Y_{JS}|^2 + \sum_{S=0}^{1} \sum_{J} \sum_{J' \neq J} |b_{JS} b^*_{J'S} Y_{JS} Y^*_{J'S}| \quad (J+J' \text{ even}), \qquad (4)$$

$$(I^+ - I^-) \sim \sum_{S=0}^{1} \sum_{J} \sum_{J' \neq J} |b_{JS} b^*_{J'S} Y_{JS} Y^*_{J'S}| \quad (J+J' \text{ odd}). \qquad (5)$$

In our earlier work for small K, the sum was approximated by the dipole cross section and the difference was terminated at $J=2$ and contained only the $(J=1)\times(J=0)$ and $(J=1)\times(J=2)$ interference terms. Experiments at two special ejected-electron directions then enabled the determination of monopole and quadrupole magnitudes and phases relative to the dipole amplitude.

For larger K it is necessary to retain more multipole amplitudes in Eqs. (4) and (5). Nevertheless, because the dipole term is still the largest, it is worthwhile to form the sum and difference spectra. The sum spectrum is dominated by the $4d^9 5s^2 5p$ dipole cross section, but the difference spectrum contains only the odd parity interference cross terms which are dependent on both the magnitude and relative phases of the multipole amplitudes. This is true even if the PWBA is inapplicable, for the following reason. The breakdown of the PWBA implies that the above relationships need to be extended to allow for all sublevels $M=-J\rightarrow J$; because of the parity favored and unfavored processes this is nontrivial. However, the parity of the Y_{JM} does not depend on M and hence the parity of the cross terms is still determined by $J+J'$. The form of Eqs. (4) and (5) is therefore similar. The sum and difference spectra in cadmium thus provide a more sensitive test of *any* theory than a direct comparison of a spectrum at a single ejected-electron direction.

We have carried out extensive pseudorelativistic Hartree-Fock (HFR) calculations [15] to model the sum and difference spectra. PWBA matrix elements have been calculated *ab initio* for autoionizing levels and appropriate continua to enable the construction of all b_{JS} for $J=0\rightarrow 7$, which proved an adequate range for $K\leqslant 1$. Since we are ignoring exchange effects, only $J=0\rightarrow 3$ autoionizing levels may be excited, and hence for $J=4\rightarrow 7$ only nonresonant ionization occurs. Autoionization is included by using Fano-type theories [1,17], in which we assume that all matrix elements are constant over the energy range of interest. The autoionizing levels are shown in Table I; with the exception of the $J=3$ levels [18], the positions of these levels are those found to give good agreement with our earlier data [8]. For the dipole and octupole ionization processes, both singlet and triplet

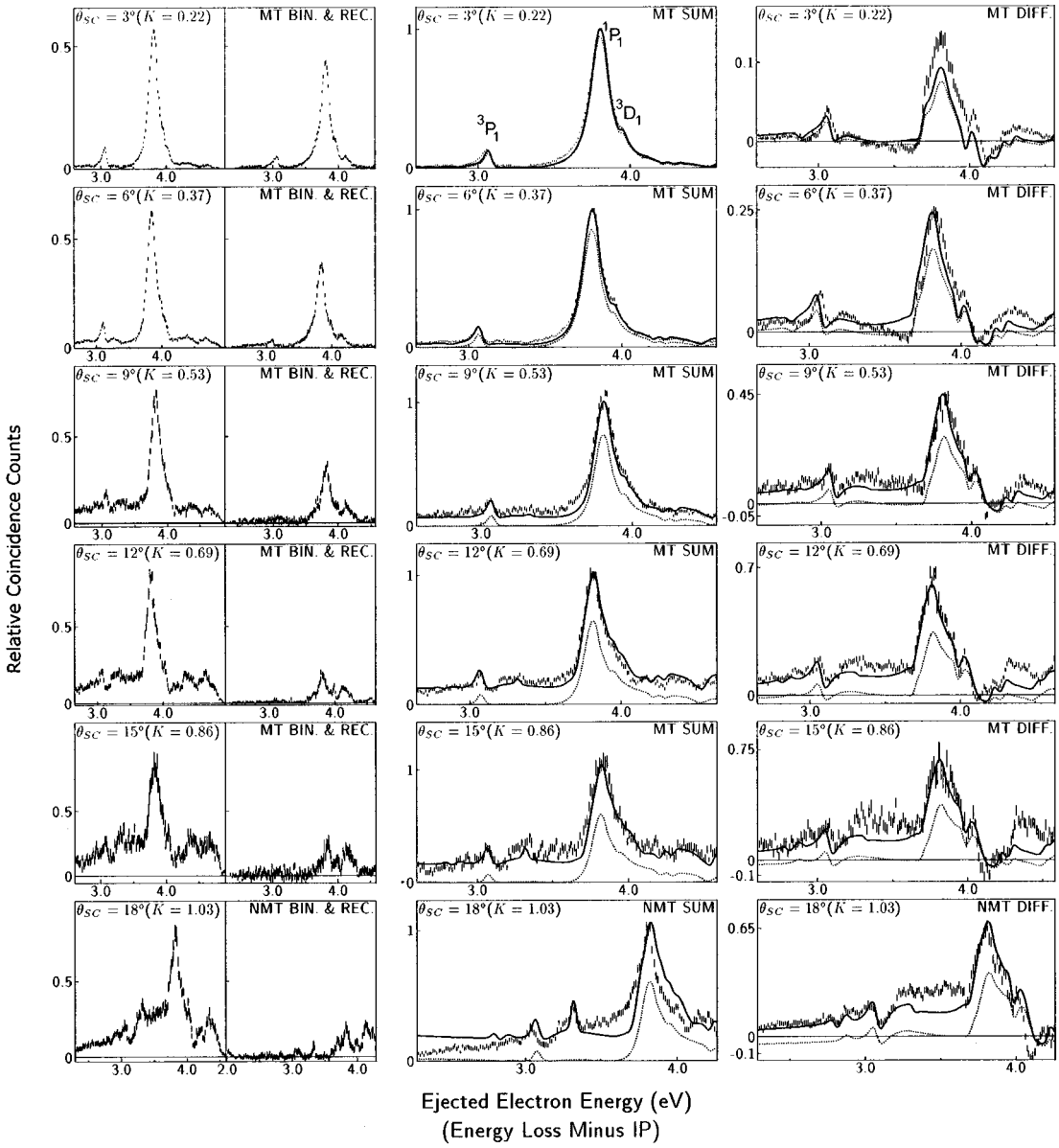

FIG. 1. Momentum-transfer axis experiments. $(e,2e)$ energy spectra for 150-eV electrons incident on atomic cadmium with scattering angles between 2° and 18°, and electrons ejected parallel (binary direction) and antiparallel (recoil direction) to the momentum-transfer direction. The vertical bars represent the statistical uncertainties. The double panels on the left are the raw spectra. The central panels show the sum and the right panels show the difference between the binary and recoil spectra; the positions of the $4d^9 5s^2 5p\ J=1$ resonances are shown in the 3° sum spectrum. The solid curves in the sum and difference spectra are PWBA calculations with partial-wave amplitudes $J=0\rightarrow 7$; the dotted curves show the contribution of $J=0\rightarrow 2$. Experiments and calculations are normalized to unity in the $4d^9 5s^2 5p\ ^1P_1$ resonance position of the sum spectra.

continua are involved; this is described in Refs. [5,18,19]. The HFR calculations show that for $J=0$ and 2 autoionizing levels there is negligible coupling to the triplet continua, and hence the monopole and quadrupole processes may be calculated from the formalism of several levels that couple to a single continuum [1]. The PWBA matrix elements involve single particle $l_i \rightarrow l_f$ reduced matrix elements [15] $\langle l_f || j_J(Kr) || l_i \rangle$, where j_J is a spherical Bessel function of order J. Details of how this is done for the various autoionizing levels is given in Ref. [8]. The complex coefficients $b_{JS}=|b_{JS}|e^{i\delta_{JS}^T}$ involve the total phase [20]

$$\delta_{JS}^T = \chi_J - \tfrac{1}{2} J\pi + \sigma_J + \delta_{JS} + \Delta_{JS}, \tag{6}$$

where σ_J is the hydrogenic Coulomb phase and δ_{JS} is the phase shift due to the unperturbed non-Coulombic ionic potential. The phase shift due to autoionization, Δ_{JS}, is the net shift due to all levels that couple to the same continuum. The collisional part of the phase is given in the PWBA by $\chi_J = J\pi/2$.

III. EXPERIMENT

The coplanar $(e,2e)$ spectrometer has been described in detail elsewhere [8,21]. It consists of four main components, an electron gun, a metal-vapor atomic beam oven, a scattered electron spectrometer, and an ejected-electron spectrometer.

The electron gun is recessed in a side arm of the vacuum chamber which enables the ejected-electron spectrometer to be positioned on both sides of the electron beam axis. Thus $(e,2e)$ spectra for two ejected-electron angles 180° apart may be taken in a single experimental run at the same value of θ_{sc}. Auger peaks in the noncoincident ejected-electron spectrum are used for energy calibration and alignment and intensity normalization; details are given in Ref. [22].

The ejected-electron detector contains a resistive anode type position-sensitive detector (PSD); this system enables useful count rates to be obtained at an energy resolution of 40 meV. During an experiment, energies and angles are scanned repetitively to minimize the effect of any drift in, for example, the electron beam intensity. Run times of about ten days are necessary in order to acquire an $(e,2e)$ spectral pair with adequate statistics.

IV. RESULTS

We have measured coplanar $(e,2e)$ energy spectra, in Cd for an incident electron-beam energy 150 eV and scattering angles $\theta_{sc}=2°-18°$, which, for the $4d^9 5s^2 5p$ region, correspond to momentum transfer $K\approx 0.2\rightarrow 1$ a.u. Each experimental run consisted of pairs of spectra for ejected-electron directions $\pm\hat{k}_{ej}$ and ejected-electron energies $E\approx 2.5\rightarrow 5$ eV. At each scattering angle, spectra were obtained for three directions $\hat{k}_{ej}$ chosen with regard to the properties of the spherical harmonics present in Eqs. (4) and (5). Table II gives the parameters of all the experiments described below.

A. Momentum-transfer axis experiments

The directions given by $\hat{k}_{ej}\cdot\hat{K}=\pm 1$ lie along the momentum transfer axis. These directions are close to the maxima in the binary and recoil lobes of the angular distribution. Interference effects are expected to be largest in this direction since all $M=0$ partial wave amplitudes are present and have their maximum values; the effects are expected to grow with K.

Figure 1 shows a representative selection of the momentum-transfer axis experiments (including the 3° experiment from [8]). The leftmost panels show the $(e,2e)$ spectra in the binary and recoil directions. The spectra show a strong dependence on scattering angle, with small differences at the smallest scattering angle and an almost vanishingly small recoil spectrum when $K=1$. The two right panels present the same data, but in the form of sum and difference spectra (and with an expanded energy scale). All spectra at a given scattering angle have been normalized to the $4d^9 5s^2 5p\,^1P_1$ maximum in the sum spectrum. It can be seen that the *shapes* of the sum and difference spectra are relatively independent of scattering angle; the large changes in the binary and recoil spectra can be ascribed to the *magnitude* of the interference effects revealed by the difference spectra, which increase from 10% at $K=0.2$ to 80% at $K=1$. The curves in the figures are PWBA calculations, normalized to the experiment at the $4d^9 5s^2 5p\,^1P_1$ maximum of the sum spectrum. In these calculations the *magnitudes* of the multipole amplitudes are fixed at their *ab initio* values.

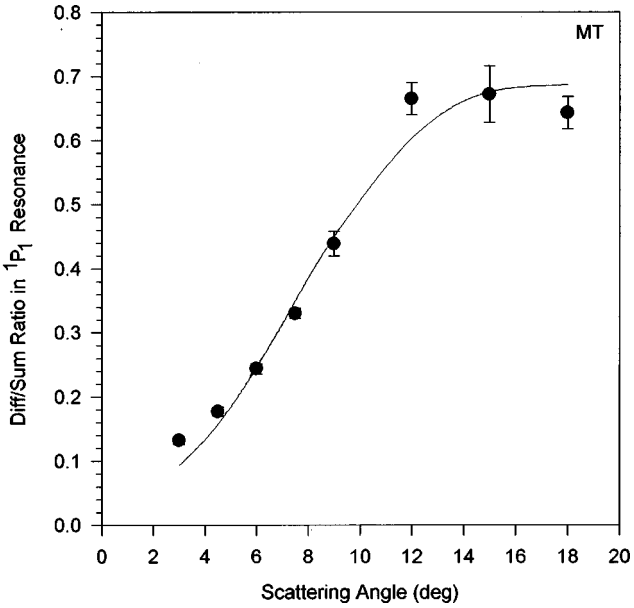

FIG. 2. Difference/sum intensity ratio at the $4d^9 5s^2 5p\,^1P_1$ resonance energy for the momentum transfer axis experiments. The solid curve is the PWBA calculation.

The *phases*, references to $J=1$, have been set as follows: for $J>2$ they are fixed at the PWBA values, but for $J=0$ and 2 they have been set at the fitted values taken from our earlier experiments. Thus $\chi_1-\chi_0$ is 0.3π less, and $\chi_1-\chi_2$ is $\pi/4$ more, than the PWBA relative phase. As can be seen from the figure, these phase corrections, obtained at small scattering angles, appear to be valid over the full range of scattering angles investigated. The solid line includes all partial waves $J=0\rightarrow 7$; the dotted line only includes $J=0\rightarrow 2$ for a comparison with our earlier work. At the larger scattering angles the $4d^9 5s^2 5p$ $J=3$ autoionizing levels can be seen in the sum spectra; this has been discussed elsewhere [18]. The main effect of the inclusion of the higher-order partial waves is the appearance of a nonzero background; the intensity of the resonance features seems relatively unaffected. The fact that the shape of the sum and difference spectra seems approximately independent of scattering angle suggests that the experiments can be usefully summarized by the value of the difference spectrum at the $4d^9 5s^2 5p\,^1P_1$ resonance. This is shown in Fig. 2 and is compared with the full PWBA calculation. The agreement between theory and the momentum-transfer experiments is remarkably good both qualitatively and quantitatively.

B. P_2 magic angle experiments

The angle defined by $\hat{k}_{ej}\cdot\hat{K}=\sqrt{1/3}$ is 54.7° away from the momentum transfer direction. We call this the P_2 magic angle, since it is the angle for which the second-order Legendre polynomial (and Y_{20}) vanishes. Thus in the PWBA the quadrupole amplitude is not present and, in our earlier experiments at small momentum transfer, we were able to extract the monopole/dipole amplitude ratio from $(e,2e)$ spectra measured at the P_2 magic angle. Although this is not possible for larger K, since $J>2$ are present, it is of interest to monitor the behavior of these spectra as the scattering

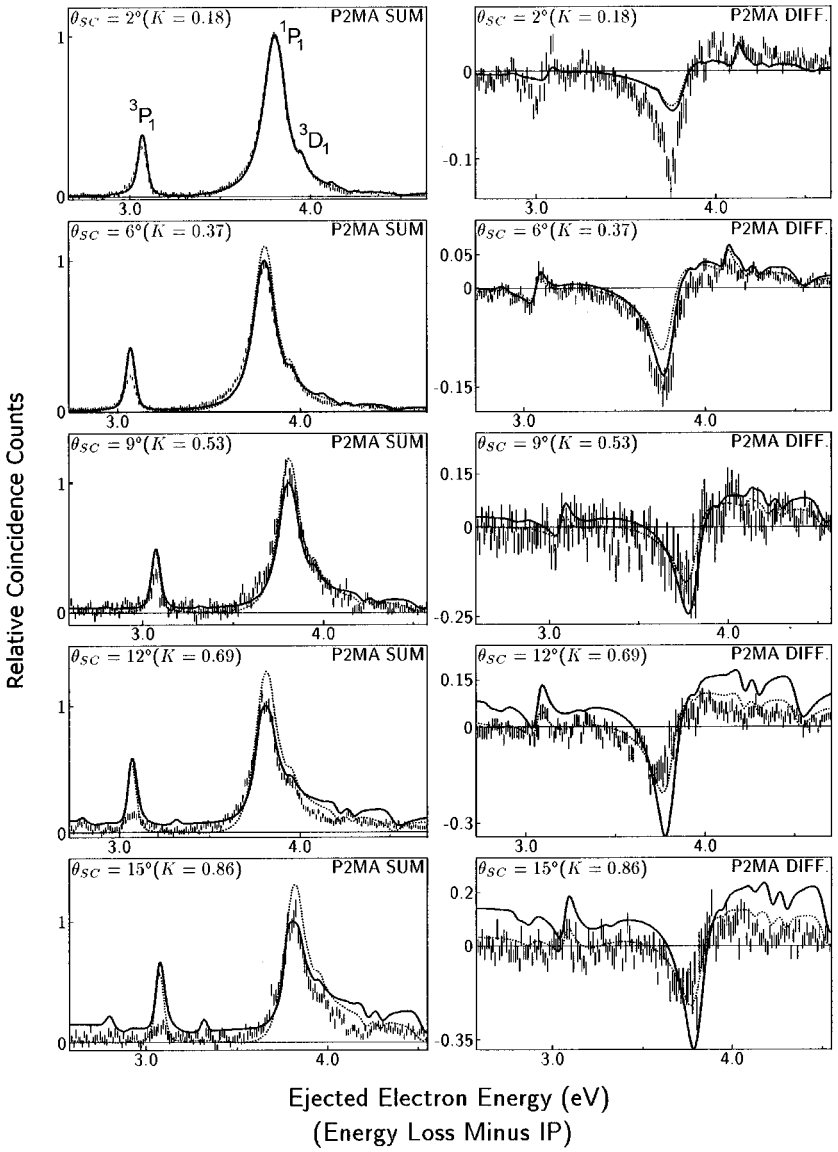

FIG. 3. P_2 magic angle experiments. As Fig. 1, showing the sum and difference spectra.

angle is increased. Figure 3 shows a representative selection of sum and difference spectra from the P_2 magic angle experiments (including the 2° experiment from Ref. [8]) compared with the PWBA calculations.

At small scattering angles the sum spectra are equivalent to the photoelectron magic angle spectra [23] and hence are proportional to the dipole photoabsorption cross section. At larger scattering angles this is only approximately true; nevertheless, two trends are apparent. First the intensity ratio of the $^3P_1/^1P_1$ decreases; this is thought to be due to electron-impact exchange processes and has been discussed elsewhere [13] (as noted above, the present PWBA calculations do not include exchange scattering). Second, the broad $^1P_1$ peak becomes asymmetric, which implies a finite Fano parameter q; the PWBA calculations are in quite good quantitative agreement, but overestimate the $J>2$ contribution to the sum spectra at the largest scattering angles.

It is remarkable that the shape of the difference spectra appears to be independent of scattering angle. We may thus summarize these spectra by the value of the minimum in the $^1P_1$ region, as is shown in Fig. 4. Even more remarkable is that the magnitude of the interference, as well as the shape,

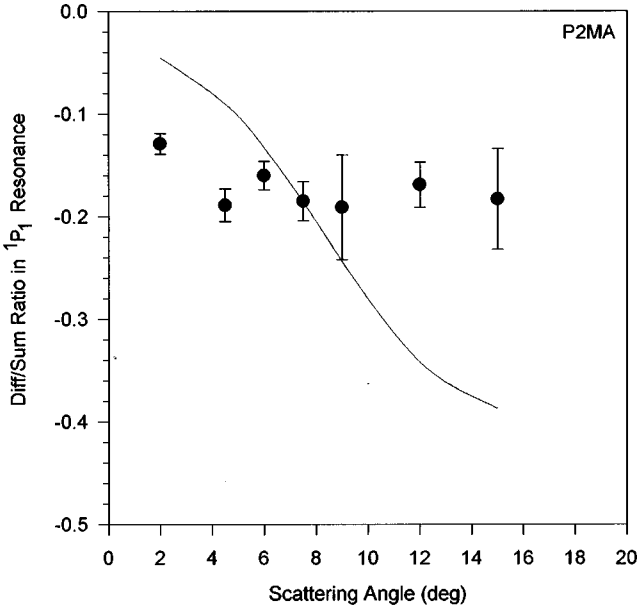

FIG. 4. As Fig. 2, for the P_2 magic angle experiments.

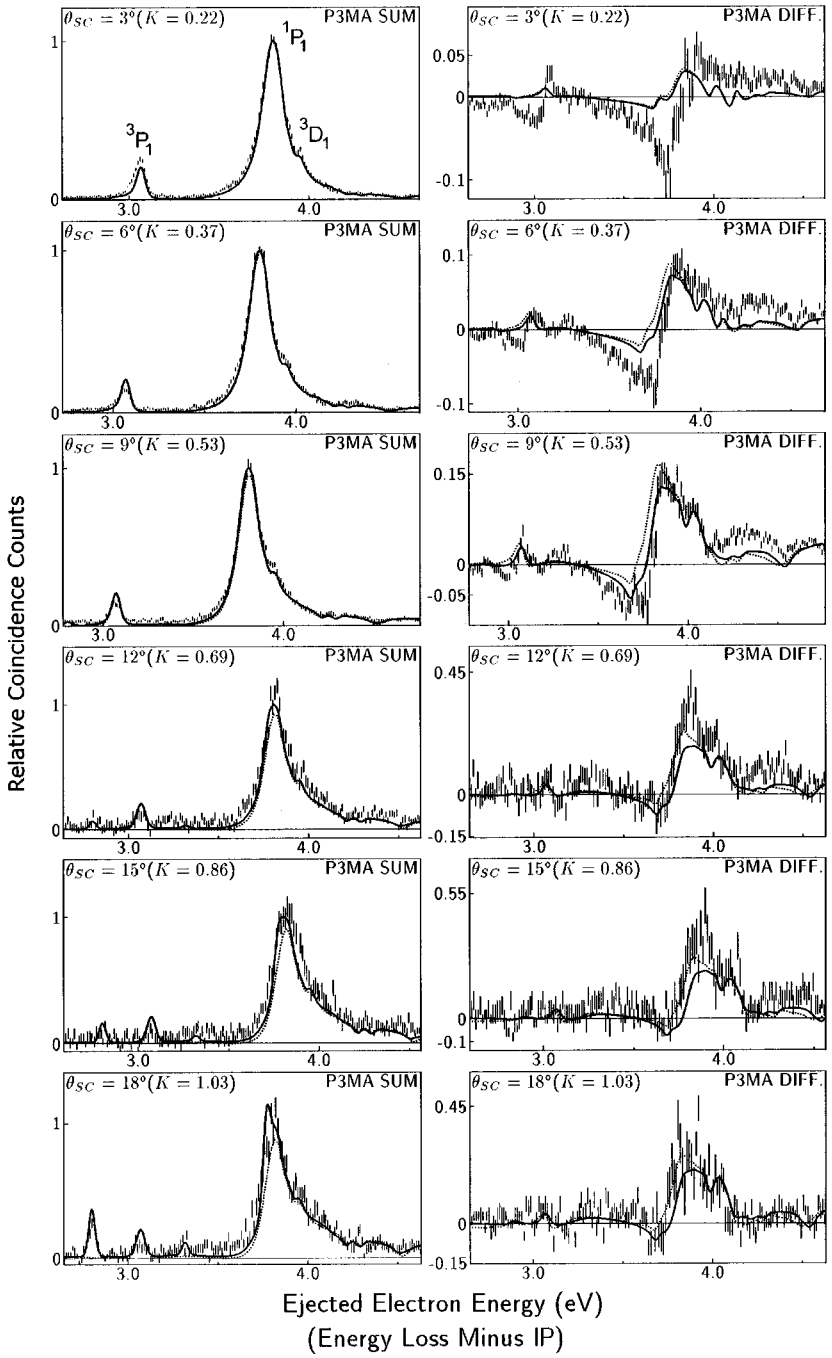

FIG. 5. P_3 magic angle experiments. As Fig. 1, showing the sum and difference spectra.

appears to be independent of scattering angle. The PWBA calculations predict the shape correctly in all cases (with the inclusion of the phase correction) but are in very poor agreement as regards the magnitude. In contrast to the momentum-transfer experiments, the inclusion of $J>2$ partial waves changes the overall magnitude of the difference spectrum (including the resonance features), but has little effect on the shape. At the smallest scattering angle the monopole/dipole magnitude ratio is 2.2 times too small [8], but at the largest scattering angle the predicted interference is about the same factor too large.

C. P_3 magic angle experiments

The angle defined by $\hat{k}_{\rm ej}\cdot\hat{K}=\sqrt{3/5}$ is 39.2° away from the momentum-transfer direction. We call this the P_3 magic angle, since it is the angle for which the third-order Legendre polynomial (and Y_{30}) vanishes, as does the contribution from the PWBA direct ionization octupole amplitude. Octupole autoionization is present, however, because the $4d^9 5s^2 5p$ $J=3$ levels are strongly parity unfavored; this has been discussed in detail elsewhere [18]. Here we note that the three levels are extremely sharp and have a very local effect. Thus, within the limitations of the PWBA, and provided K is not too large, the P_3 magic angle experiments probe the behavior of the $J=0,1,2$ partial waves with scattering angle; i.e., the regime where $J=3$ is significant but the $J>3$ partial waves are not yet important. Figure 5 shows a representative selection of sum and difference spectra from the P_3 magic angle experiments compared with the PWBA calculations.

The sum spectra show little background due to high J partial waves even at the largest scattering angle; the PWBA

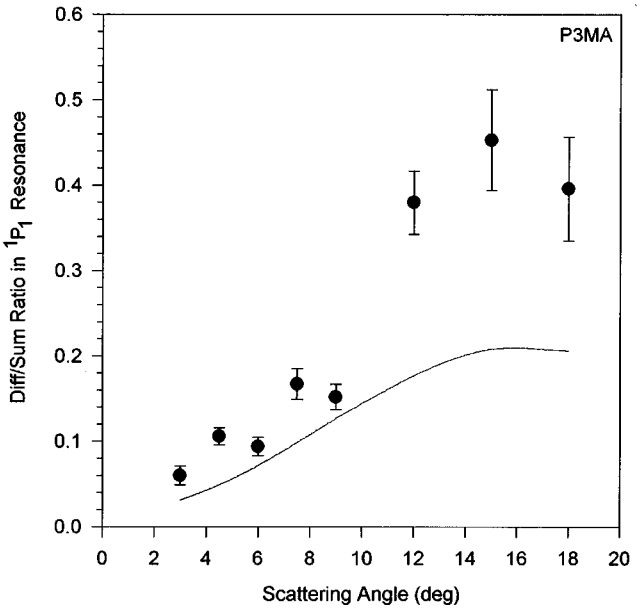

FIG. 6. As Fig. 2, for the P_3 magic angle experiments.

calculations actually predict zero background. As in the P_2 magic angle experiments, the finite q parameter for the $4d^9 5s^2 5p$ resonance is apparent.

The difference spectra show a gradual trend as the scattering angle increases: the interference maximum in the $^1P_1$ resonance region increases from 5% to 50% whereas the minimum remains approximately constant at about 7%. The PWBA, which incorporates the phase corrections, predicts the shape of the interference spectra tolerably well; it can be seen that the inclusion of $J>2$ has little effect. However, the PWBA does a poor job of predicting the magnitude, particularly at the largest scattering angles. This can be seen in Fig. 6, which shows the dependence on the scattering angle of the interference maximum.

V. DISCUSSION AND CONCLUSIONS

We have given the results of a comprehensive set of experiments on cadmium ionization by electron impact. The data have been presented in the form of sum and difference spectra, a form that highlights trends that would have been obscured had the data been given as raw $(e,2e)$ spectra. We hope these trends will provide clues for the construction of scattering calculations that involve both resonant and nonresonant ionization by electron impact in the transition from the dipole limit to the binary collision region.

It is found that within each of the three types of experiment, the *shapes* of the difference spectra are fairly independent of scattering angle. This enables all three types of experiment to be summarized in terms of the magnitude of the interference. It is remarkable that for the P_2 magic angle experiments the magnitude of the interference does not change with scattering angle, in contrast with the other two types of experiment. It is also remarkable that the PWBA is in such good agreement with the momentum-transfer experiments, but in such poor agreement with the other two types. In fact it was found impossible to adjust the PWBA magnitudes to obtain agreement with all three types of experiment. Any change that improved agreement with one type of experiment tended to worsen the agreement with the other two types.

Perhaps the most notable result of comparing the experiments with the PWBA is the fact that the $J=0,1,2$ relative phase corrections, obtained from the small-angle spectra, lead to extremely good sum and difference spectral *shapes* for all scattering angles and for all three experiment types. A possible qualitative explanation for this ''universal'' phase correction is as follows. The PWBA, by its very nature, ignores the interaction between the two outgoing electrons and hence does not incorporate a phase shift due to their interaction potential; this will be approximately spherically symmetric since it is given by a superposition of all ejected-electron partial wave amplitudes. Thus, for a fixed scattered-electron energy, the phase corrections should be approximately independent of scattering angle. We should, however, point out that for cadmium the situation is complicated by the very strong dipole transition to the bound $4d^9 5s^2 5p$ autoionizing levels, which will profoundly affect this interaction potential.

The experimental results presented here suggest the direction of future experiments. It is planned to investigate the phase corrections as a function of incident electron energy at small momentum transfer. Separate experiments will obtain coplanar $(e,2e)$ spectra at ejected-electron directions $\pm\theta$ with respect to the momentum transfer axis, for which the PWBA predicts identical spectra. Differences in the magnitude of the spectra will quantify the breakdown of the PWBA. There is also the possibility of observing PCI effects as a small shift [24] in the position of the broad Cd autoionizing resonance.

ACKNOWLEDGMENTS

This work was supported by a grant from the U.S. Department of Energy, Office of Basic Energy Sciences, Division of Chemical Sciences, Fundamental Interactions Branch, under Contract No. DE-FG05-91ER14214. M.W. acknowledges the support of the EU HCM Network Program and the U.K. PPARC.

[1] U. Fano, Phys. Rev. **124**, 1866 (1961).
[2] O. Samardzic, L. Campbell, M. J. Brunger, A. S. Kheifets, and E. Weigold, J. Phys. B **30**, 4383 (1997), and references therein.
[3] A. Crowe, D. G. McDonald, S. E. Martin, and V. V. Balashov, Can. J. Phys. **74**, 736 (1996), and references therein.
[4] M. Wilson, J. Phys. B **1**, 736 (1968).
[5] N. L. S. Martin, J. Phys. B **23**, 2223 (1990).
[6] G. V. Marr and J. M. Austin, Proc. R. Soc. London, Ser. A **310**, 137 (1969).
[7] N. L. S. Martin, D. B. Thompson, R. P. Bauman, and M.

Wilson, Phys. Rev. Lett. **72**, 2163 (1994).
[8] N. L. S. Martin, D. B. Thompson, R. P. Bauman, and M. Wilson, Phys. Rev. A **50**, 3878 (1994).
[9] D. H. Madison, V. D. Kravtsov, J. B. Dent, and M. Wilson, Phys. Rev. A **56**, 1983 (1997).
[10] N. L. S. Martin, D. B. Thompson, R. P. Bauman, C. D. Caldwell, M. O. Krause, S. P. Frigo, and M. Wilson, Phys. Rev. Lett. **81**, 1199 (1998).
[11] B. W. Shore, Phys. Rev. **171**, 43 (1968).
[12] V. V. Balashov, S. S. Lipovetsky, and V. S. Senashenko, Zh. Eksp. Teor Fiz. **63**, 1622 (1972) [Sov. Phys. JETP **36**, 858 (1973)].
[13] N. L. S. Martin, R. P. Bauman, and M. Wilson, Phys. Rev. A **57**, 1827 (1998).
[14] H. Klar, A. Franz, and H. Tenhagen, Z. Phys. D **1**, 373 (1986).
[15] R. D. Cowan, *The Theory of Atomic Structure and Spectra* (University of California Press, Berkeley, 1981).
[16] U. Fano and D. Dill, Phys. Rev. A **6**, 185 (1972); D. Dill, *ibid.* **7**, 1976 (1973).
[17] E. B. Saloman, J. W. Cooper, and D. E. Kelleher, Phys. Rev. Lett. **55**, 193 (1985); D. E. Kelleher, in *Proceedings of the 5th International Conference on Spectral Line Shapes* (De Gruyter, Berlin, 1981), p. 281, and private communication.
[18] N. L. S. Martin, R. P. Bauman, and M. Wilson, Phys. Rev. A **57**, 4346 (1998).
[19] N. L. S. Martin, Nucl. Instrum. Methods Phys. Res. B **40/41**, 228 (1989).
[20] N. L. S. Martin and D. B. Thompson, Phys. Rev. A **43,** 2281 (1991).
[21] N. L. S. Martin and D. B. Thompson, J. Phys. B **24**, 683 (1991).
[22] D. B. Thompson and N. L. S. Martin, J. Electron Spectrosc. Relat. Phenom. **77**, 277 (1996).
[23] N. L. S. Martin, D. B. Thompson, R. P. Bauman, M. Wilson, J. Jiménez-Mier, C. D. Caldwell, and M. O. Krause, J. Phys. B **27**, 3945 (1994).
[24] R. Morgenstern, A. Niehaus, and U. Thielmann, J. Phys. B **10**, 1039 (1977).